Green and Antioxidant-Functionalized MXenes: Progress, Challenges, and Applications

Fery Haidir Irawan[1], *Farah* Fahma[1*], *Lisman* Suryanegara[2], and *Khaswar* Syamsu[1]

[1]Department of Agroindustrial Technology, Faculty of Agricultural Engineering, IPB University, Bogor, West Java, Indonesia
[2]Research Center of Biomass and Bioproduct, National Research and Innovation Agency, Bogor, West Java, Indonesia

Abstract. MXenes are a family of two-dimensional transition metal carbides and nitrides ($M_{n+1}X_nT_x$) that exhibit high electrical conductivity, large surface area, and surface hydrophilicity, making them promising candidates for applications in energy storage, sensors, biomedical devices, and smart textiles. However, their synthesis commonly relies on high-level etching agents such as hydrofluoric acid (HF), raising significant concerns regarding safety and environmental sustainability. This has driven growing interest in developing green synthesis approaches that minimize toxic by-products and operational risks. Despite their functional advantages across diverse applications, MXenes face a major limitation in the form of rapid oxidation, particularly in aqueous or ambient conditions, which severely affects their durability. Surface modification using natural antioxidants, such as plant-derived polyphenols, flavonoids, and organic acids, has emerged as a green and effective strategy to enhance oxidative stability while improving biocompatibility. This review provides an overview of the current progress in green synthesis methods and antioxidant-based surface functionalization of MXenes. It also provides an overview of the potential of MXenes across diverse application domains.

1 Introduction

Since the groundbreaking discovery of graphene, the development of two-dimensional (2D) materials has progressed rapidly, introducing a wide range of structures with novel properties that form the foundation for next-generation functional technologies. MXenes, as a class of 2D transition metal carbides, nitrides, or carbonitrides, have emerged as highly promising candidates. Unlike graphene, MXenes offer competitive advantages due to their combination of exceptional properties, such as ultra-high electrical conductivity (exceeding 10,000 S cm^{-1}), comparable to metals [1], inherent hydrophilicity that enables processing in polar solvents [2], and ease of surface modification through functional groups like -OH, -O, and -F [3]. This chemical tunability facilitates the integration of MXenes with biomolecules, polymers, or inorganic compounds [4], resulting in multifunctional composites with tailored performance for specific applications.

* Corresponding author: farah_fahma@apps.ipb.ac.id

MXenes have undergone rapid advancements since their development at Drexel University in 2011. This growing interest underscores the market potential of MXenes, as the MXene Material Market is projected to grow from USD 57.7 million in 2025 to USD 437.88 million by 2034, at a compound annual growth rate (CAGR) of 25.26% [6]. MXenes are seen as a promising material for the future, with applications spanning energy storage [7], sensors [8], biomedicine [9], wearable electronics, and smart textiles [7].

Despite these exciting possibilities, conventional MXene synthesis faces considerable challenges. The use of concentrated HF to etch away the 'A' layer from MAX phases raises serious safety concerns for operators and poses environmental risks [10], thereby limiting large-scale fabrication [11]. Moreover, MXene surfaces are highly prone to oxidation, especially in aqueous and ambient environments [12], leading to structural degradation and performance deterioration.

Ongoing research is focused on overcoming these challenges by developing safer and more environmentally friendly synthesis methods that support long-term application of MXenes. The strategies to enhance the oxidative stability of MXenes include storage condition control, surface modification, and optimization of MXene structures during synthesis [13]. One particularly promising approach is the surface functionalization of MXenes with natural antioxidants, which has proven effective in prolonging material lifespan by preventing oxidative degradation [14]. This strategy aligns with green chemistry principles by avoiding toxic reagents and allowing integration of biodegradable, bio-based materials.

In line with this, the present review aims to highlight recent advancements in green synthesis techniques and antioxidant functionalization strategies for MXenes, as well as to explore their emerging applications in smart textiles, energy storage, sensing, and biomedical technologies. These approaches are anticipated to support the development of more sustainable MXene production, considering safety, material efficiency, and industrial scalability.

2 Structure of MXene

MXenes belong to a novel family of 2D-layered materials composed of transition metal carbides, nitrides, or carbonitrides [15]. As illustrated in **Fig.1.a**, the chemical elements involved in MXene synthesis are. In the periodic table, the M element (in blue) denotes early transition metals that form the backbone of the MXene structure. The A element (in pink), such as aluminum (Al) or silicon (Si), represents the atomic layer selectively etched away during the synthesis process. Meanwhile, the X element (in light green) refers to carbon and/or nitrogen atoms, which are tightly bonded to the M atoms. Common examples of M-phase transition metals include titanium (Ti), vanadium (V), chromium (Cr), niobium (Nb), and molybdenum (Mo) [16], chosen for their ability to form strong bonds with carbon and nitrogen, thus contributing to MXene's structural integrity and performance. The "X" in the MXene formula represents the carbon and/or nitrogen components of its crystal lattice [17]. The etching process specifically removes the A element, which weakens the bond between M and A layers, facilitating the generation of open and layered MXene structures through selective etching [18,19]. To date, over 340 MAX phases have been successfully identified and documented in the literature [20].

Four major structural compositions of MXenes have been successfully synthesized: M_2XT_x, $M_3X_2T_x$, $M_4X_3T_x$, and $M_5X_4T_x$ [21], as shown in **Fig. 1.b**. Based on their transition metal configurations (**Fig. 1.c**), MXenes can be classified into monometallic transition metal (TM), dual-transition metal solid-solution (DTM), ordered (DTM), and high-entropy MXenes [22]. TM MXenes consist of a single type of metal, such as Ti in $Ti_3C_2T_x$, with a general formula of $M_{n+1}X_nT_x$ and surface terminations like -OH, -O, and -F [23]. Dual-

transition metal MXenes exist in two subtypes: random solid-solution DTM, in which two different metals are randomly distributed within the lattice to allow compositional flexibility, and ordered DTM, in which the metals are arranged in alternating atomic layers, such as $Mo_2TiC_2T_x$. A more complex category includes high-entropy MXenes, which incorporate four or more transition metals in equiatomic ratios. These structures enable the stabilization of single phases and significantly broaden the structural diversity of MXenes [24]. Since their initial discovery in 2011, the MXene family has rapidly expanded to include nearly 50 distinct MXene compositions, excluding the numerous solid-solution variants and modifications achieved through surface functionalization.

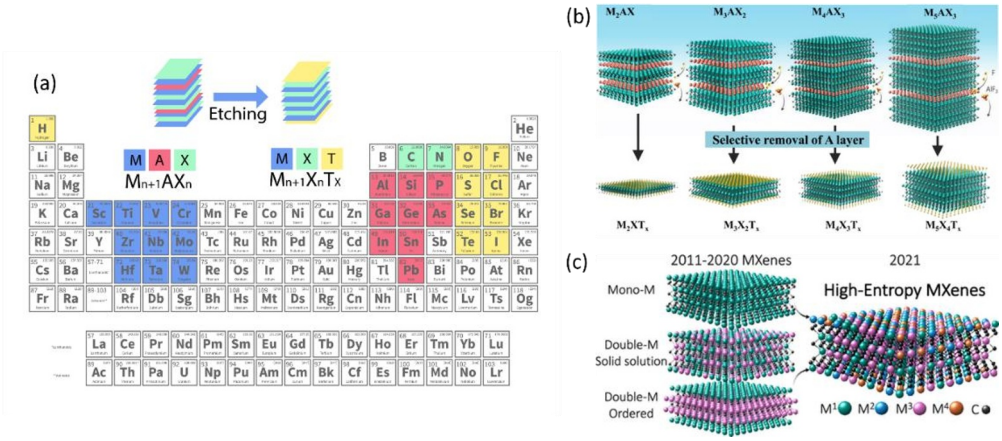

Fig. 1.a periodic table with color codes to synthesis MXene, **b** Various Mxene with $M_{n+1}X_nT_x$ formula (n=1-4) [25], **c** Mxene structure with different M-layer configuration [24]

3 Fluorine-Based Etching Synthesis of MXene

Since its discovery, MXene has been primarily synthesized via wet chemical etching using hydrofluoric acid (HF) to remove the A-layer from MAX phase precursors [26,27]. This process enables selective etching of A-group elements, facilitating the formation of open-layered MXene structures.

As illustrated in **Fig. 2.a**, Ti_3AlC_2 is treated with HF, which selectively removes the Al layer and produces a stable titanium carbide layer (Ti-C). This etching process introduces surface termination groups, such as -F and -OH, onto Ti_3C_2. Sonication is subsequently applied to exfoliate the multilayer MXene structure, yielding separated $Ti_3C_2T_x$ nanosheets. The process follows the following simplified reaction mechanisms:

$$Ti_3AlC_2 + 3HF \rightarrow AlF_3 + \frac{3}{2}H_2 + Ti_3C_2 \quad (1)$$

$$Ti_3C_2 + 2HF \rightarrow Ti_3C_2Ti_3F_2 + H_2 \quad (2)$$

$$Ti_3C_2 + 2H_2O \rightarrow Ti_3C_2(OH)_2 + H_2 \quad (3)$$

Reaction (1) shows that aluminium reacts with HF to form AlF_3, which precipitates on the MXene surface and can be removed by centrifugation or dissolved as $AlF_3.3H_2O$. Reactions (2) and (3) explain the formation of -F and -OH surface terminations, respectively.

Fig. 2.b schematically illustrates the HF etching mechanism of Ti_3AlC_2, which proceeds through: (1) grain boundary etching, (2) interlayer penetration, and (3) opening of layers. The reaction initiates at the edges and grain boundaries of bulk MAX particles, progressing inward and resulting in the formation of AlF_3 and H_2. Upon sonication, these layers delaminate into accordion-like structures of multilayer MXene.

Typically, HF-etched MXene exists in multilayer form, held together by weak van der Waals forces. Therefore, delamination is required to obtain single or few-layer MXene sheets [28], as shown in **Fig. 2.c**. Organic solvents such as dimethyl sulfoxide (DMSO) are often used for intercalation prior to sonication, enhancing layer separation [29]. Other polar solvents, including NaOH and tetrabutylammonium hydroxide (TBAOH), have also been employed. Montazeri *et al.* [28] reported that NaOH not only facilitates delamination but also better suppresses oxidation compared to TBAOH, while being significantly more cost-effective.

Despite its efficacy, the HF-based etching route presents several drawbacks. High-concentration HF (~50 wt%), prolonged reaction times, or elevated temperatures pose serious environmental and health hazards [30]. Furthermore, this process consumes substantial energy and yields MXenes with limited long-term stability. Notably, the abundant -F surface terminations generated are chemically inert, which reduces the overall reactivity and functional tunability of MXene [31].

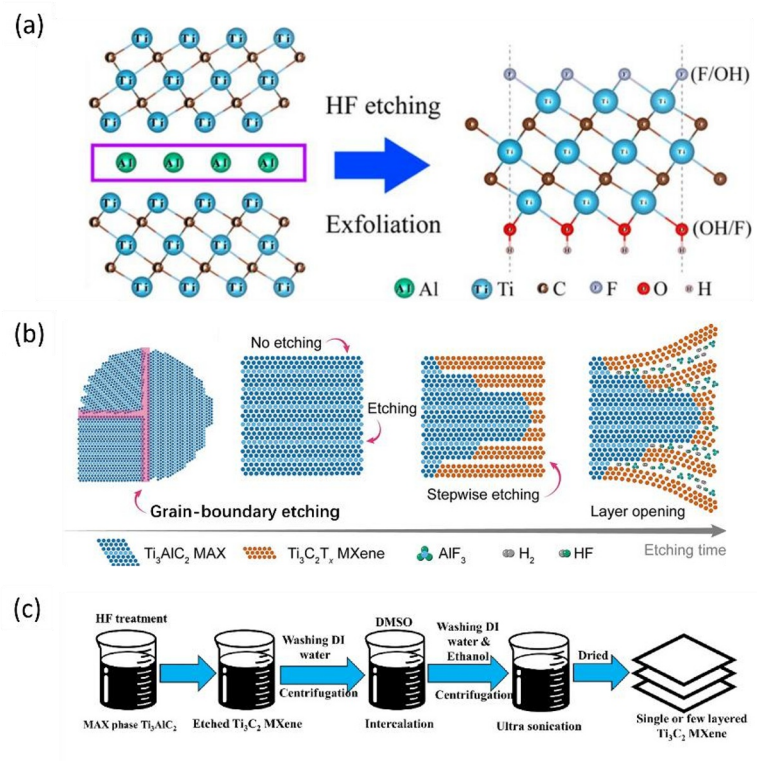

Fig. 2.a Structure of HF etching $Ti_3C_2T_x$ [32], **b** schematic of the etching process Ti_3AlC_2 MAX phase to Ti_3C_2 MXene [33], **c** MXene general process [34]

4 Synthesis of MXene via *In Situ* HF Etching

Although direct HF-based etching is highly effective in removing A-site elements from MAX phases to produce MXene, it poses significant health, environmental, and safety hazards. To address these limitations, alternative synthesis routes have been developed, including *in situ*

generation of HF. This approach reduces the direct handling of hazardous HF, replacing it with less toxic fluoride-containing precursors [35]. The *in-situ* etching proceeds via the following reaction sequence:

$$LiF + HCl \rightarrow HF + LiCl \quad (4)$$
$$Ti_3AlC_2 + 3HF \rightarrow AlF_3 + {}^{3}/_{2}\, H_2 + Ti_3C_2 \quad (5)$$
$$Ti_3C_2 + 2HF \rightarrow Ti_3C_2Ti_3F_2 + H_2 \quad (6)$$
$$Ti_3C_2{+}2H_2O \rightarrow Ti_3C_2(OH)_2 + H_2 \quad (7)$$

Moreover, the molar ratio of LiF to Ti_3AlC_2 affects the lateral size and exfoliation quality of $Ti_3C_2T_x$ MXene sheets [36]. Proper optimization of this ratio is crucial for obtaining high-quality delaminated MXene nanosheets.

However, despite its advantages, *in-situ* HF generated from HCl + LiF may not be strong enough to fully penetrate and etch all grain boundaries in polycrystalline MAX phases [37]. As a result, this method may yield a lower ratio of completely etched particles, especially in bulk or densely packed MAX powders. The efficiency of etching is therefore limited by the reaction kinetics, leading to the concept of Minimally Intensive Layer Delamination (MILD) to describe such slow and partial etching processes [35]. Additionally, although the direct handling of HF is avoided, the method still produces fluoride ions (F^-), which remain a health and environmental concern, particularly for biomedical or human-contact applications [38]. These limitations have prompted researchers to explore fluoride-free MXene synthesis techniques as a safer and greener alternative for future applications.

5 Green Synthesis of MXene Etching

Beyond improving safety, these eco-conscious methods enable the broader application of MXene in humanosphere-related domains, such as biomedical engineering, wearable electronics, and sustainable energy storage systems, where biocompatibility and low toxicity are essential [39]. Several alternative synthesis approaches have emerged as part of this movement, one of which includes alkali etching.

5.1 Alkali etching

Alkali-based etching presents a promising alternative to traditional HF etching, particularly due to the strong chemical affinity between alkali metals and aluminum (Al). While conventional halogen-based etching relies on F^- or Cl^- ions to remove the A-layer from MAX phases, alkali metals such as sodium (Na^+) or potassium (K^+) offer a fluoride-free pathway to selectively extract aluminum from Ti_3AlC_2 precursors [40]. Li *et al.* [41] demonstrated the use of sodium hydroxide (NaOH) for alkali treatment of Ti_3AlC_2. In their method, the reaction between Ti_3AlC_2, NaOH, and water leads to the formation of Ti_3C_2 MXene. During this process, Na^+ ions bind to Al, forming the soluble compound NaAlO2, which facilitates the removal of aluminum. Concurrently, Na^+ also intercalates into the Ti_3C_2 layers, contributing to the formation of -OH surface terminations through reactions with water.

The etching mechanism is highly dependent on the temperature and concentration of NaOH, with three potential reaction pathways observed. At low temperatures, aluminum tends to form insoluble Al-oxide layers (e.g., $NaAlO_2$), which hinder the efficient removal of Al and lead to incomplete etching, leaving the polycrystalline structure of Ti_3AlC_2 largely intact. Under high temperature but low NaOH concentration, partial dissolution of $Al(OH)_3$ is observed. However, the oxidation of Ti to form sodium titanate (Na-Ti-O) compounds impedes the formation of high-purity MXene. Conversely, at elevated temperatures (~270°C) and high NaOH concentrations (~27.5 M), the etching process becomes significantly more

efficient, enabling complete dissolution of aluminum as $[Al(OH)_4]^-$, and yielding cleaner MXene products.

Another study, Zhang *et al.* [42] introduced a hydrothermal-assisted alkali etching approach using a small quantity (0.7 g) of potassium hydroxide (KOH). This method successfully produced $Ti_3C_2(OH)_2$ nanoribbons (NRs), characterized by a reduced aluminium content, a high density of hydroxyl groups, and an open-layered structure. These structural features enhanced the material's electrochemical properties. Specifically, the $Ti_3C_2(OH)_2$ NRs exhibited a high specific capacity of 143.4 mAh g^{-1} at 100 mA g^{-1} after 250 charge-discharge cycles, along with excellent cycling stability and rate performance. The superior electrochemical behaviour was attributed to the nanoribbon architecture, which promotes effective ion adsorption, lithium storage, and facilitates rapid ion/electron transport. In summary, alkali etching demonstrates great potential as a green route for MXene synthesis. Alkali etching is a promising alternative to HF-based etching, offering a fluoride-free approach for MXene synthesis. However, the formation of aluminum hydroxide by-products, such as $Al(OH)_3$, can hinder the etching process and reduce the overall yield and purity of MXene.

5.2 Electrochemical etching

Electrochemical etching differs from conventional chemical etching methods, which rely on acidic or alkaline etchants to remove the A-layer from MAX phase materials to produce MXene. Electrochemical etching removes the A-phase from the MAX precursor by utilizing electrochemical principles in an electrolyte solution [43]. This etching process involves electron transfer during surface reactions, primarily driven by the chemical activity of the M-Al bond, rather than the M-C bond. In its simplest form, this method involves passing an electric current between the target material and another material within an electrochemical cell [44]. The electrochemical etching process depends on the electrolyte solution and the voltage difference applied across the electrodes [45]. The precursor is placed in an electrochemical cell, and voltage is applied between the electrodes. This application causes the metal layer to dissolve while the chalcogenide layer remains unaffected.

For the first time, Sun *et al.* [46] successfully synthesized Ti_2CT_x MXene without -F surface terminations via electrochemical etching. This process was carried out in a dilute HCl solution as the electrolyte, with a voltage of 0.6 V applied over a period of five days. The resulting MXene contained only -Cl surface groups, along with other common groups like -O and -OH. The reaction mechanisms for electrochemical etching are as follows:

$$Ti_2AlC + yCl^- + (2x + z)H_2O \rightarrow Ti_2\ C(OH)_{2x}Cl_yO_z + Al^{3+} + (x + z)H_2 + (y + 3)e^- \quad (8)$$

$$Al^{3+} + 3e^- \rightarrow Al \quad (9)$$

At the initial stage, only the surface of Ti_2AlC MAX phase interacts with the electrolyte, forming the Ti_2CT_x MXene layer. This layer eventually covers the surface and hinders further electrolyte penetration, making continued etching more difficult. Over time, the MXene layer on the surface becomes carbonized, resulting in a three-layer structure consisting of carbon, Ti_2CT_x MXene, and unetched Ti_2AlC MAX. This process results in a low MXene yield, as parameters such as electrolyte concentration, etching voltage, and duration significantly impact the final product quality [47].

Huang *et al.* [47]demonstrated electrochemical etching of Ti_3AlC_2 in a packed-bed electrochemical reactor (PBER) using NH_4F aqueous electrolyte (pH ~6.3). The MAX powder served as the anode, with platinum as the cathode (**Fig. 3.a**). The system has been scaled up to produce approximately 20 g of $Ti_3C_2T_x$ per batch (**Fig. 3.b**), with the product being delaminated using Tetramethylammonium Hydroxide (TMAOH). The galvanostatic

curve in **Fig. 3.c** shows three reaction stages: (1) anion intercalation, (2) selective etching/functionalization at 0.5-1.5 V with optimal etching rate up to 2 V, and (3) water separation at higher voltages. This operating window facilitates high etching rates. This method reduces dependence on concentrated HF, although the release of NH_3 requires monitoring due to potential environmental impact.

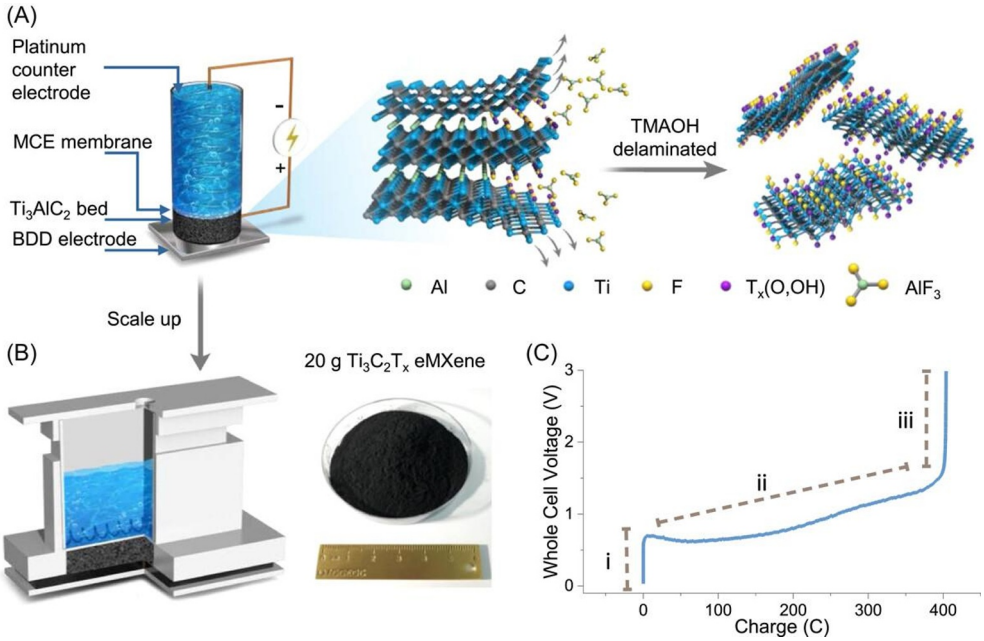

Fig. 3.a Mechanism of PBER for MXene etching, **b** scale-up PBER configuration, **c** galvanostatic charging curve of electrochemical etching stages [47].

5.3 Molten lewis-acidic etching

The molten Lewis acidic salts etching method is an alternative etching technique for MXene synthesis that utilizes molten salt as the etching medium. This etching mechanism is based on a displacement reaction between species in the molten Lewis acidic salt and the A-site atoms in the MAX precursor [48]. Li *et al.* [49] demonstrated the synthesis of MXenes through etching with molten Lewis acidic salts, such as $ZnCl_2$, as shown in **Fig. 4.a**. Sodium chloride (NaCl) and potassium chloride (KCl) are added to lower the eutectic melting point. At a temperature of 550°C, $ZnCl_2$ melts and dissociates into Zn^{2+} cations. The high electron affinity of Zn^{2+} leads to its reaction with the aluminum (Al) atoms in Ti_3AlC_2, generating Al^{3+} cations and Zn atoms. The Al^{3+} cations then bond with Cl^- anions to form $AlCl_3$, which vaporizes at 178°C. Simultaneously, Zn atoms diffuse into the Ti_3C_2 layers, replacing the Al atoms, resulting in a Ti_3ZnC_2 MXene. The reaction mechanism can be described as follows:

$$Ti_3AlC_2 + 1.5ZnCl_2 \rightarrow Ti_3C_2 + 1.5Zn + AlCl_3 \quad (10)$$

$$Ti_3C_2 + Zn \rightarrow Ti_3ZnC_2 \quad (11)$$

Li *et al.* [49] observed that when the molar ratio of Ti_3AlC_2 to $ZnCl_2$ was set to 1:6, the MAX-Zn phase underwent delamination, producing MXene terminated with Cl. Therefore, this method requires careful optimization of the molar ratio of molten salts to the MAX phase

precursor to control the number of -Cl terminations on the resulting MXene. Wei *et al.* [19] demonstrated that the molten Lewis acidic salts etching method is not limited to Al-based MAX phases but can also be applied to MAX phases containing dual or non-Al A-site elements. As shown in **Fig. 4.b**, a precursor $Ti_2(Sn_\gamma Al_{1-\gamma})C$ was used, where Sn and Al are present as A-site elements. The synthesis of MXene occurred through the selective removal of Al using the molten Lewis acidic salts, controlled by the redox potential. This process resulted in the formation of a new phase, $Ti_2Sn_\gamma CCl_x$, with a two-phase structure consisting of Ti_2SnC and Ti_2CCl_x. The etching mechanism involves the oxidation of elements at the M-sites, with the MX sublayer serving as an electron transport pathway to facilitate the oxidation of A-site elements.

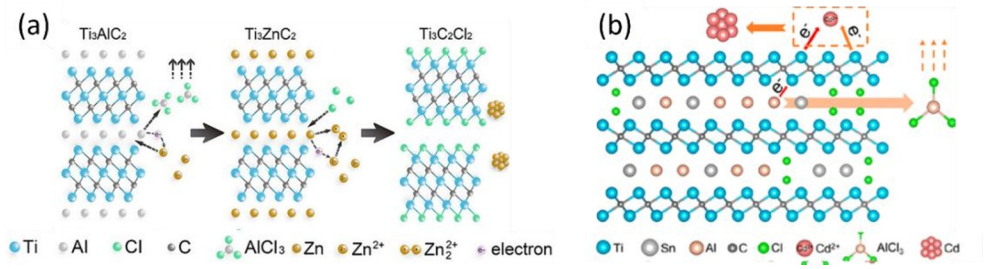

Fig. 4.a Al MAX phase, **b** Al and non-Al MAX phase Lewis acidic molten salts etching mechanisms [50].

5.4 Chemical vapor deposition (CVD) etching

In the field of ultrathin materials, Chemical Vapor Deposition (CVD) is one of the most widely used techniques for producing thin films with thicknesses down to the nanometer scale. This method works by utilizing the surface of a substrate as a site for chemical reactions. The precursors used in the CVD process must possess specific characteristics: they should be volatile enough to reach the substrate surface, have high chemical purity to avoid contamination, be stable but reactive enough to form the required layers, and pose minimal hazard during use [51]. With these characteristics, CVD not only enables the synthesis of high-quality MXenes but also offers material cost efficiency since it does not always require complex precursors.

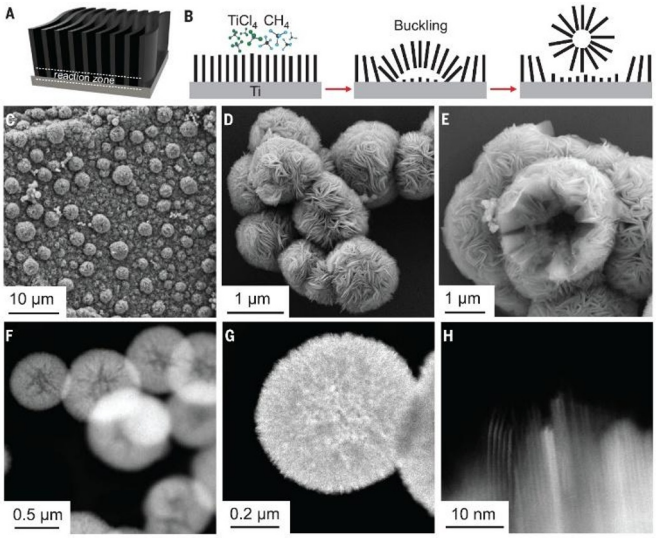

Fig. 5. Schematic diagrams illustrating the **a** reaction zone and **b** proposed buckling of microspheres CVD-Ti_2CCl_2, **c-e** SEM of morphology, **f-h** TEM morphology of CVD-Ti_2CCl_2 [52].

Wang *et al.* [52] demonstrated that CVD allows the direct synthesis of MXenes with Cl-terminations (Ti_2CCl_2) without the need for a MAX phase precursor. At high temperatures, a reaction between Ti, graphite, and $TiCl_4$ forms MXene carpets with a spherulite-like morphology. As the thickness of the growing MXene carpet increases, the diffusion of gaseous reactants toward the reaction zone slows, making the growth theoretically self-limiting, as shown in **Fig. 5.a**. However, experimental observations indicated a new growth regime that could bypass this gas diffusion bottleneck in the CVD process. The growth stages are schematically depicted in **Fig. 5.b**, which includes uniform layer formation, the emergence of "bulges" (**Fig. 5.c**), transition into spherical vesicles (**Fig. 5.**d), and the release of vesicles from the substrate (**Fig. 5.f-g**). After prolonged reaction, all Ti metal is consumed, resulting in vesicles with Ti_2CCl_2 sheets arranged radially normal to the surface (**Fig. 5.h**), with small voids at the core, as seen in fragmented vesicles and FIB-prepared samples (**Fig. 5.e**).

MXene, produced using CVD methods, yields larger dimensions (~100 μm) compared to those obtained through chemical etching (~10 μm). Although CVD is an effective synthesis method for MXenes, it typically produces thicker MXenes (~100μm) compared to the chemical etching method (~10μm), and reduces their light transmission, limiting their use in transparent materials. To address the reduction in light transmission, Kang *et al.* [53] reported the synthesis of ultrathin (5μm) and thermally stable Mo_2C-graphene (Mo_2C-Gr) hybrid films via a one-step CVD method (**Fig. 6.a**). This hybrid film, with a work function between graphene and pure Mo_2C, was chosen as the transparent hole-transport layer in a Mo_2C–Gr/$Sb_2S_{0.42}Se_{2.58}$/TiO_2/FTO two-sided photodetector (**Fig. 6.b-c**). This device could detect light from both sides, demonstrating a very fast response time (0.084 ms) and recovery time (0.100 ms), highlighting the promising potential

Despite the advantages of CVD, such as not requiring MAX phase precursors, the technique is limited by the need for high-cost equipment and significant energy consumption. These factors pose challenges to its industrial-scale implementation, indicating a need for more efficient and cost-effective alternatives to support large-scale MXene production.

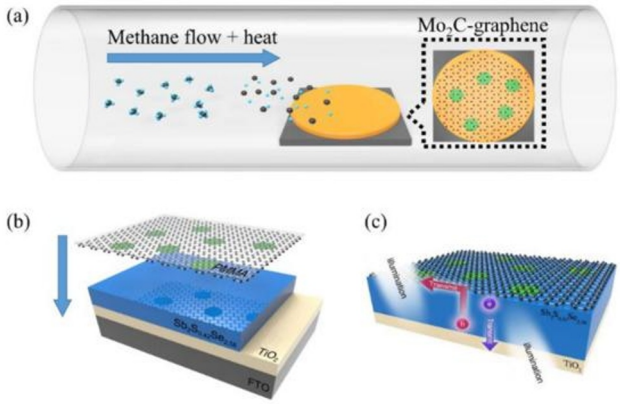

Fig. 6. The illustration of **a** crystal growth, **b** crystal transfer layer, and **c** photodetector application of Mo_2C-Gr [53].

6 Oxidation of MXene

As a promising next-generation material, MXene faces a significant challenge in terms of oxidation stability. This limitation restricts its long-term application potential, particularly in environments that require prolonged material durability. Oxidation in MXene not only disrupts its characteristic 2D properties but also degrades its physicochemical attributes, which are critical for its functionality [54]. As shown in **Fig.7.a-d**, the conductivity of MXene decreases when exposed to various media, including air and solid forms such as ice and polymers. Visual observations of the oxidation process are illustrated in **Fig.7.e**, while additional UV-Vis spectral analysis (**Fig.7.f**) further corroborates the evidence of degradation, ultimately diminishing the long-term functionality of the material.

Habib *et al.* [55] quantified the degree of oxidation in MXene films by measuring the electrical conductivity of vacuum-filtered $Ti_3C_2T_x$ films. Over a two-month exposure period to air, these films exhibited a sharp decline in conductivity, reaching approximately 7% of the initial value after 27 days ($2.49 \times 10^4 \pm 1.16 \times 10^3$ S m^{-1}), indicating rapid oxidation. When stored in the form of ice, the samples retained their conductivity better than those in liquid media, suggesting that lower temperatures and solid media slow down the oxidation rate. Furthermore, $Ti_3C_2T_x$ PVA composites (10-90 wt%) showed a similar trend to the air-exposed films, experiencing a rapid decrease in conductivity during the first four weeks, followed by a slower decline. This suggests that while solid media can slow down the oxidation process, complete prevention of degradation remains unachievable.

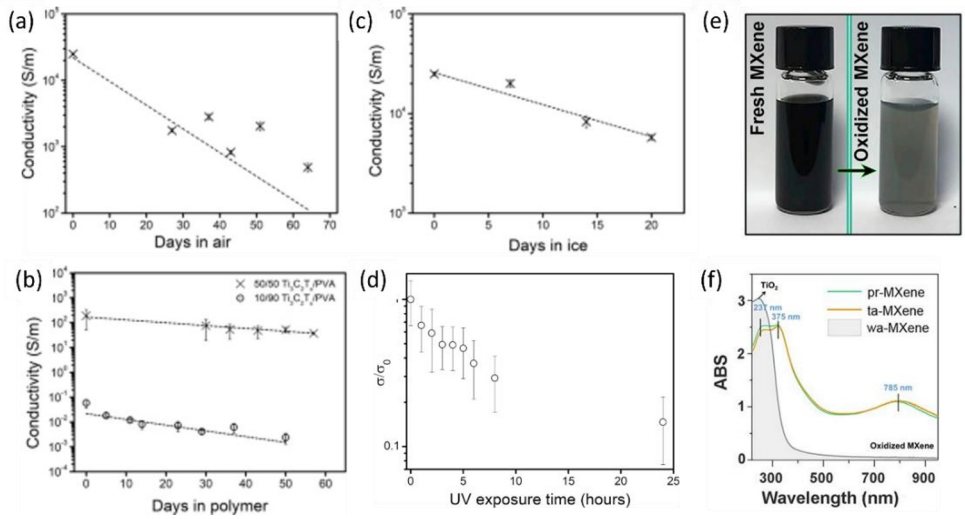

Fig. 7.MXene film conductivity characteristic in various media **a** air , **b** ice, **c** poly-vinyl alcohol (PVA), and **d** with increasing UV exposure time [55], **e** The visual and UV-Vis Spectra absorbances change of MXene aging for 7 days [56].

The high reactivity of MXene toward oxidation is often attributed to the abundance of oxygen in the atmosphere, although the detailed mechanism remains under debate [57]. The oxidation mechanism in the air atmosphere, as shown in **Fig.8.**, indicates that at the initial stage (a,b), the fresh MXene sheets remain intact with a thin, flat structure, showing no degradation. After 7 days (c,d), ultrathin anatase TiO_2 nanoparticles form on the MXene surface and later shrink laterally. After 30 days (e,f), the Ti layer directly transforms into crystalline rutile nanosheets, indicating extensive oxidation, where the MXene layers no longer retain their 2D characteristics but instead disintegrate into a mixture of disordered carbon and TiO_2 particles. Therefore, surface functionalization techniques, such as antioxidant modification, could play a crucial role in enhancing the MXene's stability and expanding its applicability in various industries.

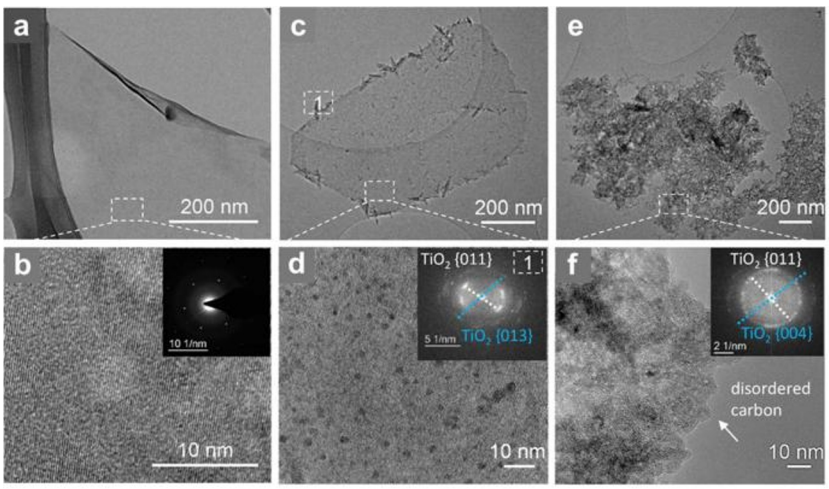

Fig. 8. TEM of MXene flakes exposed to air **a** 0 days, **c** 7 days, **e** 30 days, and b, d, f the high-resolution TEM of panels a, c, and e, respectively [58].

7 Improvement of Oxidation Stability Strategy with Antioxidant Functionalization

The oxidation stability of MXene in its original colloidal form is a critical aspect for expanding its applications. The oxidation mechanism in aqueous media has proven to be complex, with the rate influenced by various factors ranging from the intrinsic composition of MXene to the conditions of its colloidal environment. Initially, dissolved oxygen was considered the primary factor, but recent studies emphasize the dominant role of water in the hydrolysis process of MXene [57]. Consequently, scientific attention is increasingly focused on developing strategies to enhance the oxidation stability of MXene colloids, with promising new approaches being reported to slow down or suppress degradation.

Several strategies have been developed to reduce the oxidation rate during storage in colloidal form, thus extending the service life of MXene-based devices. Oxidation suppression in MXene can also be achieved through surface modification, such as utilizing reductive diamines that serve as both intercalators and grafting agents [59]. One strategy that has gained significant attention for improving the oxidation resistance of MXene is surface modification with antioxidant agents [60]. This approach is considered relatively simple and efficient, providing a practical pathway to prolong the shelf life of MXene in its aqueous colloidal form without compromising its functional properties.

Antioxidants are defined as compounds that have the ability to slow down, delay, or inhibit the oxidation process of a substrate (**Fig. 9.a**) [61]. A systematic study on the antioxidant performance of various organic compounds with similar structures indicates that the chelation effect between antioxidant molecules and cation of metals atoms is likely a key factor contributing to the enhanced stability of the material [62]. However, not all antioxidants have a positive effect; some may be neutral or even accelerate the oxidation process. This is reflected in the graph of Ti^{4+} ion content in the aqueous MXene suspension, with an average of about 48%, as shown in **Fig. 9.b**. Among the compounds tested, oxalic acid and citric acid were found to be the most effective in improving the oxidative stability of MXene. The diversity in antioxidant molecular structures leads to varying effects on MXene, underscoring the need for systematic analysis to understand the chemical interaction mechanisms between the two.

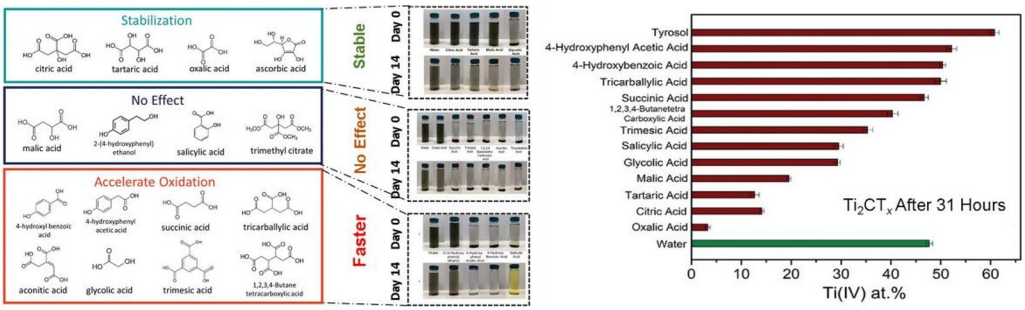

Fig. 9.a Antioxidant categories and their effect on the oxidation stability of MXene suspensions over 14 days, **b** XPS measurement of MXene to atoms percentage of Ti^{4+} [63].

8 Antioxidant Surface Functionalization of MXene Application

The development of antioxidant-modified MXene opens new opportunities for expanding its applications across various functional fields. Functionalization with antioxidant molecules not only enhances the oxidation resistance of MXene but also enriches its chemical and physical properties, such as electrochemical stability, biocompatibility, and the ability to interact with target ions or molecules. With protection against degradation, antioxidant-modified MXene can be utilized more effectively in energy applications (supercapacitors, batteries), smart textiles, and biomedical systems. Therefore, this approach is considered strategic in overcoming the limitations of pure MXene while broadening its potential applications.

Zhang *et al.* [56] developed a MXene/PEDOT:PSS supercapacitor electrode modified with tartaric acid as an antioxidant. The modification was carried out by immersing the film in a 50 wt% tartaric acid solution for 5 minutes at 90°C. The results showed a fourfold increase in conductivity, high water stability, and an areal capacitance (CA) of 1.149 μF cm^{-2}, surpassing other 2D material-based systems. High-frequency performance was demonstrated with an 80° phase angle at 120 Hz and an RC time constant of 263 μs, making it ideal for AC line-filtering applications. Long-term stability was maintained with a capacitance retention of 98% after 10,000 cycles, proving the effectiveness of antioxidant functionalization in improving MXene's performance and durability. Although modification with tartaric acid improves its stability in aqueous colloids above 60°C, further analysis is needed regarding the thermal stability of the MXene/PEDOT:PSS tartaric acid-modified material for supercapacitor applications, considering the potential use of MXene in high-temperature energy systems.

As a further development, Lee *et al.* [64] developed of MXene stabilization using tartaric acid (TA), structural modification was carried out by forming composites with TEMPO-oxidized cellulose nanofiber (TOCN). This strategy aimed to enhance MXene's oxidation stability and mechanical strength while maintaining sufficient conductivity for electrochemical applications. **Fig. 10.a** shows the layered structure of the MXene/TOCN/TA composite film, where hydrogen bonding and coordination between the carboxyl groups of TOCN and TA with Ti atoms on the MXene surface form a chemically stable network. Visually, oxidation stability is shown in **Fig. 10.b**, where the MXene/TOCN/TA composite retains the characteristic dark color of MXene after 7 days in a 0.2 wt% H_2O_2 solution, unlike pure MXene, which undergoes significant color changes due to oxidative degradation. Mechanical durability tests through ultrasonic treatment for 5 minutes (**Fig. 10.c**) show that the composite film remains intact, while the pure MXene film degrades, indicating improved cohesive strength. The addition of TOCN and TA reduces the electrical conductivity of the film, as shown in **Fig. 10.d**, but the conductivity remains within functional ranges for flexible device applications. Moreover, thermogravimetric analysis (TGA) reveals that MXene/TOCN or MXene/TOCN/TA composites exhibit lower thermal stability compared to pure MXene composites. This is because TA and TOCN exhibit low thermal stability, with decomposition temperatures of 252°C and 307°C, respectively. However, MXene/TA only lost 5.7% of its mass, indicating strong interfacial bonding between TA and MXene.

On the other hand, Guo *et al.* [65] designed MXene-based hybrid network composites modified with hyaluronic acid (HA) and hyperbranched polysiloxane (HSi) for long-term thermal camouflage applications. HA serves as an effective antioxidant agent stabilizing the MXene structure against oxidative degradation without affecting its infrared camouflage performance. Meanwhile, HSi molecules act as crosslinking agents, creating a stable and cohesive composite network. The MXene/HA/HSi composite exhibits flexible mechanical properties, high resistance to water, solvents, and extreme environmental conditions, and low infrared emissivity (±0.29). This composite can be applied to textiles via a simple, large-scale

spraying method and demonstrates resistance to environmental exposure for up to approximately 8 months. Its potential applications are highly relevant in defense and medical fields, particularly as a coating material for infrared radiation protection or thermal camouflage.

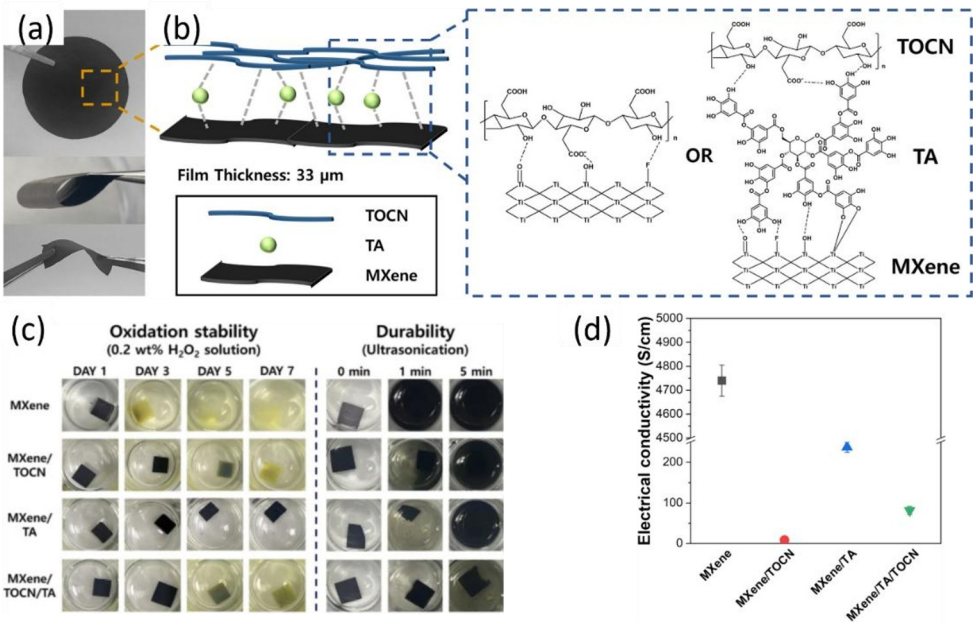

Fig.10. a Mxene-Tannic acid (TA)-TEMPO cellulose nanofiber (TOCN) composites, **b** chemical structure MXene-TA-TOCN, **c** Oxidative stability test, and **d** Electrical conductivity of MXenes [64]

The transition to smart textiles marks a significant expansion in the potential applications of MXene-based materials. In efforts to create multifunctional smart textiles, Yan *et al.* [66] modified MXene nanosheets with gallic acid (GA) and Fe^{3+} ions to produce materials with high stability and superior thermal and electromagnetic performance. As shown in **Fig. 11.a**, MG (MXene@GA) was regularly arranged on carbon fibers (CCF) through initial Fe^{3+} complexation, forming strong and stable bonds. GA interacts with the MXene surface via coordination and hydrogen bonds (**Fig. 11.b**), while Fe^{3+} acts as a bridge between MG and CCF, creating a robust laminated structure. GA's protection against MXene oxidation is demonstrated in **Fig. 11.c**, where its dispersion remains stable after 30 days, in contrast to pure MXene, which degrades and forms dark precipitates. For electromagnetic applications, **Fig. 11.d** shows that only the CCF-Fe-MG textile exhibits high EMI shielding efficiency, with a value greater than 35 dB in the X-band frequency range. Its heating ability is also responsive, as shown in **Fig. 11.e**, where the temperature increases from 28°C to 116°C under a gradual voltage of 1-8 V. Furthermore, Fig. 11f reveals the thermal camouflage effect, where, despite a high actual temperature, infrared imaging shows a lower temperature due to the low IR emissivity of MXene, providing an advantage for temperature camouflage in open environments.

Another researcher, Deng *et al.* [67], developed multifunctional textiles based on MXene/tannic acid-modified cellulose nanofibers (TACNF) using a screen-printing method and post-printing treatment with Zinc chloride (ZnCl2). The presence of phenolic hydroxyl groups in tannic acid (TA) acts as an effective antioxidant agent to prevent MXene degradation. Meanwhile, the metal coordination process between Zn ions and TA molecules generates a cross-linked network that enhances the structural stability of the functional layers

on the textile. This composite not only shows significant antimicrobial activity against Escherichia coli and Staphylococcus aureus but also has adequate electrical conductivity for detecting both micro and macro human movement variations. Moreover, its high photothermal and electrothermal conversion capabilities extend its application prospects in thermal therapy, heat sterilization, and the development of responsive smart healthcare textiles.

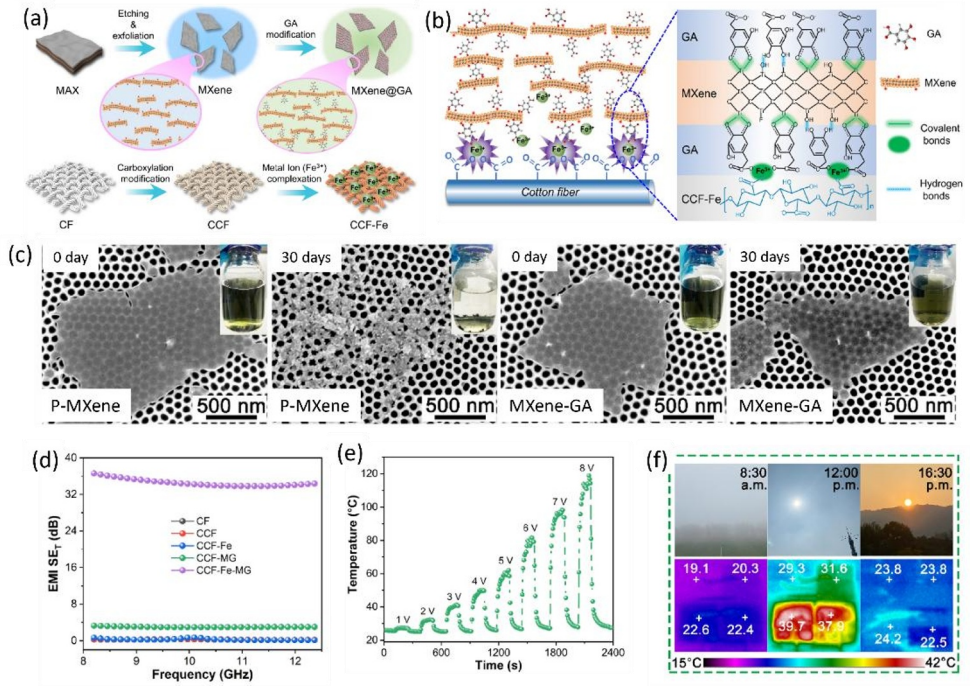

Fig. 11. a MXene-gallic acid (MG) with metal ion decoration onto a textile, **b** Chemical bonding mechanism of cotton fabric-decorated metal-MG (CCF-Fe-MG), **c** SEM of pristine MXene and MG stored at room temperature, **d** Electromagnetic interference (EMI) shielding test of MXene, **e** Joule heating performance at different voltages of CCF-Fe-MG, **f** Direct thermal camouflage and thermal image of CCF-Fe-MG [66].

Various studies above highlight the vast potential applications of antioxidant-modified MXene, which not only acts as a stabilizer against oxidation but also enhances the functionality of the material across various fields. As radical scavengers, antioxidants possess specific capabilities that are particularly relevant in the healthcare and food sectors. Therefore, it is crucial to further analyze how modifying MXene with antioxidants not only extends shelf life and structural stability but also opens new application opportunities in fields such as medicine, smart textiles, active food packaging, and sustainable energy systems.

9 Challenges and Future Outlook

9.1 Challenges

Although MXene has garnered significant attention due to its multifunctional properties, its widespread application still faces several technical and practical challenges. One of the main challenges lies in the development of environmentally friendly synthesis processes to replace conventional acid fluoride (HF)-based etching methods. While these approaches are safer

and potentially more sustainable, methods like alkaline etching still show low production yields. On the other hand, techniques like electrochemical etching and chemical vapor deposition (CVD) require high operational costs and infrastructure that has not yet been widely standardized, limiting the efficiency and scalability of the processes.

Furthermore, efforts to stabilize MXene through antioxidant functionalization have emerged as a promising alternative strategy to address oxidative degradation. Antioxidants such as tannic acid, gallic acid, or other polyphenolic compounds have been shown to extend the shelf life and maintain the structural stability of MXene, both in suspension and solid forms. However, the challenge lies in the limited comprehensive studies on the impact of these modifications on MXene's functional properties in various application contexts. In some cases, functionalization may alter the active surface of MXene, which plays a crucial role in conductivity, photothermal interaction, or sensor sensitivity, necessitating further exploration of the additional functional effects of antioxidant functionalization, particularly in more diverse MXene applications.

Moreover, the scalability and industrial application of antioxidant-modified MXene still require thorough evaluation. While this functionalization method is relatively simple, the development of ready-to-use formulations in solid forms, such as films, membranes, or composites, is still limited. There are a few reports that test the economic feasibility, long-term durability, and material performance in real-world environments, such as high temperatures, extreme humidity, or exposure to other active compounds. Therefore, the development of formulation strategies and testing the material's durability under various application conditions becomes a critical challenge before this material can be widely used in energy, healthcare, and smart textile fields.

9.2 Future outlook

The future development of MXene heavily relies on surface engineering strategies and the sustainability of its synthesis processes. One promising approach is the utilization of specific termination groups (T_x), such as -OH, -F, -O, and -Cl, which can be tailored to direct the functional properties of MXene towards specific applications. These termination groups play a crucial role in influencing conductivity, hydrophilicity, binding capacity, and oxidative stability, enabling more precise engineering of MXene for fields such as flexible electronics, biomedical sensors, and electromagnetic shielding.

Additionally, the integration of green synthesis approaches based on biomass in the etching and stabilization processes of MXene is becoming increasingly relevant, not only to improve resource efficiency but also to open up significant opportunities for the development of sustainable applications. The use of bio-based sources, either as etching agents or stabilizers, not only reduces reliance on corrosive chemicals like HF but also results in MXene materials that are more environmentally friendly and compatible with human health. One strategy that is being increasingly explored is the modification of MXene with antioxidant compounds, which has proven to be a simple yet effective way to enhance oxidative stability and expand the material’s functionality. This approach holds potential for scaling up to industrial levels, but it still requires in-depth studies on economic feasibility, long-term durability, and performance evaluation under real-world application conditions. In particular, it is important to explore the application forms of modified MXene in solid or composite forms, rather than just in suspension. This is crucial to support the implementation of MXene technology in the form of coatings, films, or more stable and applicable composite material structures for functional devices.

Acknowledgment

The authors gratefully acknowledge the Directorate General of Research and Development, Ministry of Education, Science, and Technology of Indonesia for sponsoring the conference fee under the Research Program Implementation Contract of 2025 (Contract No. 006/C3/DT.05.00/PL/2025).

References

1. K. Hantanasirisakul and Y. Gogotsi, Electronic and Optical Properties of 2D Transition Metal Carbides and Nitrides (MXenes). Advanced Materials. **30**, (2018). https://doi.org/10.1002/adma.201804779
2. H. Zhou, F. Wang, Y. Wang, C. Li, C. Shi, Y. Liu, and Z. Ling, Study on contact angles and surface energy of MXene films. RSC Adv. **11**, 5512 (2021). https://doi.org/10.1039/D0RA09125A
3. W. Huang, J. Wang, W. Lai, and M. Guo, MXene Surface Architectonics: Bridging Molecular Design to Multifunctional Applications. Molecules. **30**, 1929 (2025). https://doi.org/10.3390/molecules30091929
4. M. Mozafari and M. Soroush, Surface functionalization of MXenes. Mater Adv 2. **7277** (2021). https://doi.org/10.1039/D1MA00625H
5. Industryresearch.biz, *Mxene Material Market Overview* (2025). https://www.industryresearch.biz/market-reports/mxene-material-market-107859
6. C. Deng, S. Zhao, E. Su, Y. Li, and F. Wu, Trilayer MXene Fabric for Integrated Ultrasensitive Pressure Sensor and Wearable Heater. Adv Mater Technol. **6** (2021). https://doi.org/10.1002/admt.202100574
7. N. Alanazi, T. Selvi Gopal, M. Muthuramamoorthy, A. A. E. Alobaidi, R. A. Alsaigh, M. H. Aldosary, S. Pandiaraj, M. Almutairi, A. N. Grace, and A. Alodhayb, Cu_2O/MXene/rGO Ternary Nanocomposites as Sensing Electrodes for Nonenzymatic Glucose Sensors. ACS Appl Nano Mater. **6**, 12271 (2023). https://doi.org/10.1021/acsanm.3c01959
8. H. Wang, J. Sun, L. Lu, X. Yang, J. Xia, F. Zhang, and Z. Wang, Competitive electrochemical aptasensor based on a cDNA-ferrocene/MXene probe for detection of breast cancer marker Mucin1. Anal Chim Acta. **1094**, 18 (2020). https://doi.org/10.1016/j.aca.2019.10.003
9. I.-W. P. Chen, A. A. Kashale, and Y.-H. Pan, Hydrofluoric Acid-Free Synthesis of $Ti_3C_2T_x$ MXene Nanostructures for Energy Applications. ACS Appl Nano Mater. **6**, 1985 (2023). https://doi.org/10.1021/acsanm.2c04948
10. M. A. Zaed, J. Paul, S. Aktar, J. Jacob, K. H. Tan, and P. Thomas, A comprehensive analysis on feasibility and economic viability of commercial-scale MXene synthesis. Energy Nexus. **21**, 100625 (2026). https://doi.org/10.1016/j.nexus.2025.100625
11. Z. Khalid, F. Hadi, J. Xie, V. Chandrabose, and J. Oh, The Future of MXenes: Exploring Oxidative Degradation Pathways and Coping with Surface/Edge Passivation Approach. Small. **21**, (2025). https://doi.org/10.1002/smll.202407856
12. Y. Li, Y. Li, L. Zhao, S. Chen, S. Guo, X. Yang, P. Wang, K. Li, F. Lei, W. Feng, Z. Mou, and H. Wei, Recent progress in the antidegradation strategies of two-dimensional transition metal carbides (MXenes). J Environ Chem Eng. **12**, 112762 (2024). https://doi.org/10.1016/j.jece.2024.112762
13. Y. Wei, P. Zhang, R. A. Soomro, Q. Zhu, and B. Xu, Advances in the Synthesis of 2D MXenes. Advanced Materials. **33**, (2021). https://doi.org/10.1002/adma.202103148

14. H. Vadakke Neelamana, S. M. Rekha, and S. V. Bhat, Ti 3 C 2 T *x* MXene: A New Promising 2D Material for Optoelectronics. Chem of Mater. **35**, 7386 (2023). https://doi.org/10.1021/acs.chemmater.3c01660
15. Z. Sofer, X. Wang, and M. Yu, MXene Chemistry and Applications. Small Methods. **7**, (2023). https://doi.org/10.1002/smtd.202300778
16. A. Sinha, Dhanjai, H. Zhao, Y. Huang, X. Lu, J. Chen, and R. Jain, MXene: An emerging material for sensing and biosensing. TrAC Trends in Analytical Chem. **105**, 424 (2018). https://doi.org/10.1016/j.trac.2018.05.021
17. S. Bagheri, A. Lipatov, N. S. Vorobeva, and A. Sinitskii, Interlayer Incorporation of A-Elements into MXenes Via Selective Etching of A′ from $M_{n+1}A'_{1-x}A''_xC_n$ MAX Phases. ACS Nano. **17**, 18747 (2023). https://doi.org/10.1021/acsnano.3c02198
18. H. Wei, L. Chen, H. Ding, Y. Li, Z. Chai, and Q. Huang, Dual-Phase Structure through Selective Etching of the Double A-Element MAX Phase in Lewis Acidic Molten Salts. J Phys Chem Lett. **15**, 4486 (2024). https://doi.org/10.1021/acs.jpclett.4c00785
19. R. M. Snyder, T. Nguyen, P. Bhatt, A. A. Riaz, P. K. Thakur, T.-L. Lee, A. Regoutz, A. K. Jones, and C. S. Birkel, $(V_{1-y}Mo_y)_2CT_x$ MXene Nanosheets as Electrocatalysts for Hydrogen Evolution. ACS Appl Nano Mater. **8**, 1137 (2025). https://doi.org/10.1021/acsanm.4c06029
20. S. Zhang, G. Zhang, L. Fang, Z. Wang, F. Wu, G. Liu, Q. Wang, and H. Nian, Surface-Modification Strategy to Produce Highly Anticorrosive Ti3C2Tx MXene-Based Polymer Composite Coatings: A Mini-Review. Materials. **18**, 653 (2025). https://doi.org/10.3390/ma18030653
21. A. A. P. R. Perera, K. A. U. Madhushani, B. T. Punchihewa, A. Kumar, and R. K. Gupta, MXene-Based Nanomaterials for Multifunctional Applications. Materials. **16**, 1138 (2023). https://doi.org/10.3390/ma16031138
22. R. Ibragimova, P. Erhart, P. Rinke, and H.-P. Komsa, Surface Functionalization of 2D MXenes: Trends in Distribution, Composition, and Electronic Properties. J Phys Chem Lett. **12**, 2377 (2021). https://doi.org/10.1021/acs.jpclett.0c03710
23. S. K. Nemani, B. Zhang, B. C. Wyatt, Z. D. Hood, S. Manna, R. Khaledialidusti, W. Hong, M. G. Sternberg, S. K. R. S. Sankaranarayanan, and B. Anasori, High-Entropy 2D Carbide MXenes: $TiVNbMoC_3$ and $TiVCrMoC_3$. ACS Nano. **15**, 12815 (2021). https://doi.org/10.1021/acsnano.1c02775
24. V. A. Tran, N. T. Tran, V. D. Doan, T.-Q. Nguyen, H. H. Pham Thi, and G. N. L. Vo, Application Prospects of MXenes Materials Modifications for Sensors. Micromachines (Basel). **14**, 247 (2023). https://doi.org/10.3390/mi14020247
25. T. Kvashina, N. Uvarov, and A. Ukhina, Synthesis of Titanium Carbide by Means of Pressureless Sintering. Ceramics. **3**, 306 (2020). https://doi.org/10.3390/ceramics3030028
26. A. Jawaid, A. Hassan, G. Neher, D. Nepal, R. Pachter, W. J. Kennedy, S. Ramakrishnan, and R. A. Vaia, Halogen Etch of Ti 3 AlC 2 MAX Phase for MXene Fabrication. ACS Nano. **15**, 2771 (2021). https://doi.org/10.1021/acsnano.0c08630
27. K. Montazeri, H. Badr, K. Ngo, K. Sudhakar, T. Elmelegy, J. Uzarski, V. Natu, and M. W. Barsoum, Delamination of MXene Flakes Using Simple Inorganic Bases. The Journal of Physical Chemistry C. **127**, 10391 (2023). https://doi.org/10.1021/acs.jpcc.3c02318
28. G. Lv, J. Wang, Z. Shi, and L. Fan, Intercalation and delamination of two-dimensional MXene (Ti3C2Tx) and application in sodium-ion batteries. Mater Lett. **219**, 45 (2018). https://doi.org/10.1016/j.matlet.2018.02.016
29. K. Mahabari, R. D. Mohili, M. Patel, A. H. Jadhav, K. Lee, and N. K. Chaudhari, HF-free microwave-assisted synthesis of MXene as an electrocatalyst for hydrogen

evolution in alkaline media. Nanoscale Adv. **6**, 5388 (2024). https://doi.org/10.1039/D4NA00250D

30. A. Zamhuri, G. P. Lim, N. L. Ma, K. S. Tee, and C. F. Soon, MXene in the lens of biomedical engineering: synthesis, applications and future outlook. Biomed Eng Online. **20**, 33 (2021). https://doi.org/10.1186/s12938-021-00873-9
31. M. Tang, J. Li, Y. Wang, W. Han, S. Xu, M. Lu, W. Zhang, and H. Li, Surface Terminations of MXene: Synthesis, Characterization, and Properties. Symmetry (Basel). **14**, 2232 (2022). https://doi.org/10.3390/sym14112232
32. M. Anayee, C. E. Shuck, M. Shekhirev, A. Goad, R. Wang, and Y. Gogotsi, Kinetics of Ti_3AlC_2 Etching for $Ti_3C_2T_x$ MXene Synthesis. Chem of Mater. **34**, 9589 (2022). https://doi.org/10.1021/acs.chemmater.2c02194
33. R. Verma, A. Sharma, V. Dutta, A. Chauhan, D. Pathak, and S. Ghotekar, Recent trends in synthesis of 2D MXene-based materials for sustainable environmental applications. Emergent Mater. **7**, 35 (2024). https://doi.org/10.1007/s42247-023-00591-z
34. J.-C. Lei, X. Zhang, and Z. Zhou, Recent advances in MXene: Preparation, properties, and applications. Front Phys (Beijing). **10**, 276 (2015). https://doi.org/10.1007/s11467-015-0493-x
35. C. Wang, S. Chen, and L. Song, Tuning 2D MXenes by Surface Controlling and Interlayer Engineering: Methods, Properties, and Synchrotron Radiation Characterizations. Adv Funct Mater. **30**, (2020). https://doi.org/10.1002/adfm.202000869
36. H. Kang, L. Han, S. Chen, S. Xie, M. Li, Q. Fang, and S. He, Research Progress on Two-Dimensional Layered MXene/Elastomer Nanocomposites. Polymers (Basel) 14, 4094 (2022). https://doi.org/10.3390/polym14194094
37. X. Xu, Y. Zhang, H. Sun, J. Zhou, F. Yang, H. Li, H. Chen, Y. Chen, Z. Liu, Z. Qiu, D. Wang, L. Ma, J. Wang, Q. Zeng, and Z. Peng, Progress and Perspective: MXene and MXene-Based Nanomaterials for High-Performance Energy Storage Devices. Adv Electron Mater. **7**, (2021). https://doi.org/10.1002/aelm.202000967
38. T. Amrillah, C. Abdullah, A. Hermawan, F. Sari, and V. Alviani, Towards Greener and More Sustainable Synthesis of MXenes: A Review. Nanomaterials. **12**, 4280 (2022). https://doi.org/10.3390/nano12234280
39. Z. Sun, R. Wang, V. E. Matulis, and K. Vladimir, Structure, Synthesis, and Catalytic Performance of Emerging MXene-Based Catalysts. Molecules. **29**, 1286 (2024). https://doi.org/10.3390/molecules29061286
40. T. Li, L. Yao, Q. Liu, J. Gu, R. Luo, J. Li, X. Yan, W. Wang, P. Liu, B. Chen, W. Zhang, W. Abbas, R. Naz, and D. Zhang, Fluorine-Free Synthesis of High-Purity $Ti_3C_2T_x$ (T=OH, O) via Alkali Treatment. Angewandte Chemie International Edition. **57**, 6115 (2018). https://doi.org/10.1002/anie.201800887
41. B. Zhang, J. Zhu, P. Shi, W. Wu, and F. Wang, Fluoride-free synthesis and microstructure evolution of novel two-dimensional $Ti_3C_2(OH)_2$ nanoribbons as high-performance anode materials for lithium-ion batteries. Ceram Int. **45**, 8395 (2019). https://doi.org/10.1016/j.ceramint.2019.01.148
42. N. Li, J. Huo, Y. Zhang, B. Ye, X. Chen, X. Li, S. Xu, J. He, X. Chen, Y. Tang, Y. Zhu, K. Ling, and R. Zhu, Transition metal Carbides/Nitrides (MXenes): Properties, synthesis, functional modification and photocatalytic application. Sep Purif Technol. **330**, 125325 (2024). https://doi.org/10.1016/j.seppur.2023.125325
43. V. Sharma, D. Kumar Das, R. K. Gupta, G. Yasin, and A. Kumar, Synthesis strategies and structural and electronic properties of MXenes-based nanomaterials for ORR: A mini review. Inorg Chem Commun. **141**, 109496 (2022). https://doi.org/10.1016/j.inoche.2022.109496

44. M. Mudassar Aslam, T. Noor, and N. Iqbal, Advances in MXenes synthesis and MXenes derived electrocatalysts for oxygen electrode in metal-air batteries: A review. Materials Science and Engineering: B 292, 116400 (2023). https://doi.org/10.1016/j.mseb.2023.116400
45. W. Sun, S. A. Shah, Y. Chen, Z. Tan, H. Gao, T. Habib, M. Radovic, and M. J. Green, Electrochemical etching of Ti_2AlC to Ti_2CT_x (MXene) in low-concentration hydrochloric acid solution. J. Mater. Chem. A 5, 21663 (2017). https://doi.org/10.1039/C7TA05574A
46. Z. Huang, J. Qin, Y. Zhu, K. He, H. Chen, H. Y. Hoh, M. Batmunkh, T. M. Benedetti, Q. Zhang, C. Su, S. Zhang, and Y. L. Zhong, Green and scalable electrochemical routes for cost-effective mass production of MXenes for supercapacitor electrodes. Carbon Energy. **5**, (2023). https://doi.org/10.1002/cey2.295
47. P. Huang and W.-Q. Han, Recent Advances and Perspectives of Lewis Acidic Etching Route: An Emerging Preparation Strategy for MXenes. Nanomicro Lett. **15**, 68 (2023). https://doi.org/10.1007/s40820-023-01039-z
48. M. Li, J. Lu, K. Luo, Y. Li, K. Chang, K. Chen, J. Zhou, J. Rosen, L. Hultman, P. Eklund, P. O. Å. Persson, S. Du, Z. Chai, Z. Huang, and Q. Huang, Element Replacement Approach by Reaction with Lewis Acidic Molten Salts to Synthesize Nanolaminated MAX Phases and MXenes. J Am Chem Soc. **141**, 4730 (2019). https://doi.org/10.1021/jacs.9b00574
49. S. Kim, H. Jo, J. Yun, J.-W. Lee, J. Cho, K. Kang, and H.-D. Lim, Sustainable and eco-friendly syntheses of green MXenes for advanced battery applications. Nano Converg. **12**, 39 (2025). https://doi.org/10.1186/s40580-025-00504-2
50. M. Jussambayev, K. Shakenov, S. Sultakhan, U. Zhantikeyev, K. Askaruly, K. Toshtay, and S. Azat, MXenes for sustainable energy: A comprehensive review on conservation and storage applications. Carbon Trends. **19**, 100471 (2025). https://doi.org/10.1016/j.cartre.2025.100471
51. D. Wang, C. Zhou, A. S. Filatov, W. Cho, F. Lagunas, M. Wang, S. Vaikuntanathan, C. Liu, R. F. Klie, and D. V. Talapin, Direct synthesis and chemical vapor deposition of 2D carbide and nitride MXenes. Science (1979). **379**, 1242 (2023). https://doi.org/10.1126/science.add9204
52. Z. Kang, Z. Zheng, H. Wei, Z. Zhang, X. Tan, L. Xiong, T. Zhai, and Y. Gao, Controlled Growth of an Mo_2C—Graphene Hybrid Film as an Electrode in Self-Powered Two-Sided Mo_2C—Graphene/$Sb_2S_{0.42}Se_{2.58}$/TiO_2 Photodetectors. Sensors. **19**, 1099 (2019). https://doi.org/10.3390/s19051099
53. S. Sunderiya, S. Suragtkhuu, S. Purevdorj, T. Ochirkhuyag, M. Bat-Erdene, P. Myagmarsereejid, A. D. Slattery, A. S. R. Bati, J. G. Shapter, D. Odkhuu, S. Davaasambuu, and M. Batmunkh, Understanding the oxidation chemistry of Ti3C2T (MXene) sheets and their catalytic performances. Journal of Energy Chem. **88**, 437 (2024). https://doi.org/10.1016/j.jechem.2023.09.037
54. T. Habib, X. Zhao, S. A. Shah, Y. Chen, W. Sun, H. An, J. L. Lutkenhaus, M. Radovic, and M. J. Green, Oxidation stability of Ti3C2Tx MXene nanosheets in solvents and composite films. NPJ 2D Mater Appl. **3**, 8 (2019). https://doi.org/10.1038/s41699-019-0089-3
55. M. Zhang, F. Héraly, M. Yi, and J. Yuan, Multitasking tartaric-acid-enabled, highly conductive, and stable MXene/conducting polymer composite for ultrafast supercapacitor. Cell Rep Phys Sci. **2**, 100449 (2021). https://doi.org/10.1016/j.xcrp.2021.100449
56. R. A. Soomro, P. Zhang, B. Fan, Y. Wei, and B. Xu, Progression in the Oxidation Stability of MXenes. Nanomicro Lett. **15**, 108 (2023). https://doi.org/10.1007/s40820-023-01069-7

57. C. J. Zhang, S. Pinilla, N. McEvoy, C. P. Cullen, B. Anasori, E. Long, S.-H. Park, A. Seral-Ascaso, A. Shmeliov, D. Krishnan, C. Morant, X. Liu, G. S. Duesberg, Y. Gogotsi, and V. Nicolosi, Oxidation Stability of Colloidal Two-Dimensional Titanium Carbides (MXenes). Chemistry of Materials. **29**, 4848 (2017). https://doi.org/10.1021/acs.chemmater.7b00745
58. M. Peng, L. Wang, L. Li, X. Tang, B. Huang, T. Hu, K. Yuan, and Y. Chen, Manipulating the Interlayer Spacing of 3D MXenes with Improved Stability and Zinc-Ion Storage Capability. Adv Funct Mater. **32**, (2022). https://doi.org/10.1002/adfm.202109524
59. X. Wang, Z. Wang, and J. Qiu, Stabilizing MXene by Hydration Chemistry in Aqueous Solution. Angewandte Chemie International Edition. **60**, 26587 (2021). https://doi.org/10.1002/anie.202113981
60. A.-M. Chiorcea-Paquim, Electrochemistry of Flavonoids: A Comprehensive Review. Int J Mol Sci. **24**, 15667 (2023). https://doi.org/10.3390/ijms242115667
61. K. Ajisaka, Y. Oyanagi, T. Miyazaki, and Y. Suzuki, Effect of the chelation of metal cation on the antioxidant activity of chondroitin sulfates. Biosci Biotechnol Biochem. **80**, 1179 (2016). https://doi.org/10.1080/09168451.2016.1141036
62. X. Zhao, H. Cao, B. J. Coleman, Z. Tan, I. J. Echols, E. B. Pentzer, J. L. Lutkenhaus, M. Radovic, and M. J. Green, The Role of Antioxidant Structure in Mitigating Oxidation in $Ti_3C_2T_x$ and Ti_2CT_x MXenes. Adv Mater Interfaces. **9**, (2022). https://doi.org/10.1002/admi.202200480
63. Y. Lee, Y. Hong, and B. S. Shim, Bio-inspired reinforcement of MXene composites: tannic acid and TEMPO-oxidized cellulose nanofibers for enhanced mechanical and oxidation stability. Macromol Res. **33**, 1085 (2025). https://doi.org/10.1007/s13233-025-00395-6
64. B. Guo, Y. Wang, C. Cao, Z. Qu, J. Song, S. Li, J. Gao, P. Song, G. Zhang, Y. Shi, and L. Tang, Large-Scale, Mechanically Robust, Solvent-Resistant, and Antioxidant MXene-Based Composites for Reliable Long-Term Infrared Stealth. Advanced Science. **11**, (2024). https://doi.org/10.1002/advs.202309392
65. B. Yan, X. Bao, Y. Gao, M. Zhou, Y. Yu, B. Xu, L. Cui, Q. Wang, and P. Wang, Antioxidative MXene@GA-Decorated Textile Assisted by Metal Ion for Efficient Electromagnetic Interference Shielding, Dual-Driven Heating, and Infrared Thermal Camouflage. Advanced Fiber Materials. **5**, 2080 (2023). https://doi.org/10.1007/s42765-023-00330-3
66. P. Deng, N. Li, Y. Feng, Z. Liu, C. Lu, and Z. Zhou, Antioxidant MXene/TA/Nanocellulose Hybrid Ink for Screen Printing of Multifunctional Smart Textiles with Enhanced Antibacterial Performance. Ind Eng Chem Res. **64**, 1597 (2025). https://doi.org/10.1021/acs.iecr.4c03699